Journal of Dentistry 90 (2019) 103213

Contents lists available at ScienceDirect

Journal of Dentistry

journal homepage: www.elsevier.com/locate/jdent

Measurement of the shrinkage of natural and simulated lesions on root surfaces using CP-OCT

Vincent Yang[a], Daniel Fried[b,*]

[a] University of California, San Francisco, San Francisco, CA 94143-0758, United States
[b] Division Biomaterials and Bioengineering, Department of Preventive and Restorative Dental Sciences, University of California, San Francisco, 707 Parnassus Ave., San Francisco, CA 94143-0758, United States

ARTICLE INFO

Keywords:
Optical coherence tomography
Root caries
Shrinkage
Lesion activity

ABSTRACT

Objectives: Demineralized root dentin and cementum is made up of mostly collagen that shrinks significantly upon dehydration or drying with air. During remineralization mineral is deposited on the outside of the lesion creating a highly mineralized surface layer that inhibits diffusion, arrests the lesion and prevents shrinkage. Previous studies suggest that active root caries lesions manifest shrinkage, while arrested lesions no longer manifest shrinkage upon dehydration. The purpose of this study was to demonstrate that the shrinkage of root caries lesions can be monitored during dehydration using an optical coherence tomography probe suitable for clinical use.

Methods: In this *in vitro* study the shrinkage of simulated and natural root caries lesions on extracted teeth was measured using a cross polarization optical coherence tomography (CP-OCT) system and a 3D printed appliance with an integrated air nozzle suitable for clinical use. Two methods were employed to assess shrinkage, changes in the position of the lesion surface and changes in the thickness of the lesion.

Results: CP-OCT was successful in measuring a significant ($P < 0.05$) contraction of the lesion surface, significant decrease in the lesion thickness and increase in the reflectivity per micron upon drying natural lesions on extracted teeth.

Conclusions: In this preclinical study, we have demonstrated that a CP-OCT handpiece modified for infection control with an attached air nozzle suitable for *in vivo* use can be used to monitor the shrinkage of root caries lesions. In addition, we have developed a new approach to measuring lesion shrinkage with OCT, namely monitoring changes in the lesion thickness as opposed to the position of the lesion surface, that does not require an initial reference position and is more easily implemented *in vivo*.

1. Introduction

Clinical diagnosis of root caries is highly subjective and is based on visual and tactile parameters. In contrast to coronal caries, root caries lacks a valid diagnostic standard, such as radiography [1]. Moreover, early root caries lesions are much more difficult to detect than the early incipient white spot lesions seen with coronal caries. There are often no clinical symptoms with root caries, although pain may be present in advanced lesions. Traditional methods of visual-tactile diagnosis for root caries can result in a correct diagnosis, but not until the lesion is at an advanced stage [1]. In addition, investigators have not developed a reliable relationship between lesion appearance and activity [2–4]. Even though most experts agree that active root lesions are soft, tactile hardness assessments remain subjective and lack reliability [2]. Multifactorial root caries scoring systems have been developed with mixed success [5,6]. More recently, the International Caries Detection and Assessment System (ICDAS) coordinating committee and Ekstrand et al. proposed clinical scoring systems for assessing root caries lesion activity [5,7]. Criteria include: color (light /dark brown, black); Texture (smooth, rough); Appearance (shiny or glossy, matte or non-glossy); Tactile (soft, leathery, hard); Cavitation (loss of anatomical contour); and proximity to the gingival margin [8]. However, such clinical methods for root caries lesion activity assessment lack histological validation and are composed of only visual and tactile exams, which are prone to subjective bias and interference from staining [9]. Histological analyses for lesion assessment such as transverse microradiography (TMR) and polarized light microscopy (PLM) require destruction of the tooth and are not suitable for use *in vivo*. Incorrect diagnosis can result in under treatment or over treatment. If a decision to restore is made prematurely when remineralization was feasible, the patient is

* Corresponding author.
E-mail address: daniel.fried@ucsf.edu (D. Fried).

https://doi.org/10.1016/j.jdent.2019.103213
Received 2 August 2019; Received in revised form 8 October 2019; Accepted 12 October 2019

committed to a restoration, or replacement restorations, that can become progressively larger. If the lesion is active and intervention is delayed, often the patient will require a root canal or extraction.

Accurate diagnosis of early root caries and non-carious cervical lesions will allow clinicians to apply appropriate treatments for occlusion of dentinal tubules and restoration of the lost tooth structure. If lesions are detected early enough, they can likely be arrested/reversed by non-surgical means through chemical intervention and dietary changes [1]. Accurate determination of the degree of lesion activity and severity is of paramount importance for accurate diagnosis, risk assessment, and effective intervention. Many lesions have been arrested and will likely not benefit from intervention. Reliable methods are needed to assess lesion activity. The use of CP-OCT during lesion dehydration offers the potential for lesion activity assessment at a single time-point and, if necessary, monitoring with repeated assessments since no ionizing radiation is used. CP-OCT is uniquely capable of showing structural changes such as the formation of a zone of increased mineral density and reduced light scattering due to remineralization that indicate that the lesion is arrested [10–12]. The formation of a distinct transparent surface zone [11,13] has also been established.

Although the penetration depth of near-IR light is limited in dentin compared to enamel, high quality images of early root caries and demineralization in dentin are feasible [14]. CP-OCT has been used successfully to measure demineralization in simulated caries models in dentin and on root surfaces (cementum) [12,15,16]. CP-OCT has also been used to measure remineralization on dentin surfaces and to detect the formation of a highly mineralized layer on the lesion surface after exposure to a remineralization solution [16]. Cementum has lower reflectivity than dentin in OCT images, making it possible to easily discriminate the remaining cementum thickness [15,16]. OCT has also been used to help discriminate between noncarious cervical lesions and root caries *in vivo* [17]. Kaneko et al. and Zakian et al. [18,19] demonstrated that lesions on coronal surfaces could be differentiated from sound enamel in thermal images. Thermal imaging *via* dehydration can also be used to assess lesion activity on both enamel [20] and dentin [21] surfaces.

OCT is ideally suited for measuring dimensional changes in the tooth. Shrinkage occurs in demineralized dentin and cementum due to the loss of water from the collagen with dehydration. More severe lesions manifest greater shrinkage while lesions that have been successfully remineralized and have formed an intact highly mineralized surface zone have reduced shrinkage [16]. There is a correlation between the lesion severity and the degree of shrinkage measured using OCT [15]. Upon remineralization, such lesions expanded to the original contours and no longer manifested shrinkage [15]. This suggests that the degree of shrinkage of root caries lesions can serve as an indicator of severity and help discriminate between active and arrested root caries lesions. Recently the shrinkage of natural caries lesions on extracted teeth was measured with OCT [22]. In this study, we used a 3D printer to print an appliance that was attached to a CP-OCT handpiece for the *in vivo* monitoring of shrinkage and tested the device on both simulated and natural lesions on root surfaces. Two methods were employed to assess shrinkage, changes in the position of the lesion surface and changes in the thickness of the lesion.

2. Methods

2.1. Sample preparation

Teeth extracted from patients in the San Francisco Bay Area were collected, cleaned, sterilized with gamma radiation, and stored in a 0.1% Thymol solution. These teeth were then sliced into < 0.5 mm slices in the axial direction leaving the root surface exposed and these slices were halved in the apical direction. These slices were examined to make sure that there were no natural lesions or calculus on them. These slices were mounted on 1.2×3 cm rectangular blocks of black orthodontic composite resin with the outward tooth dentin surface facing up. The root surface was covered with acid-resistant varnish, nail polish from Revlon (New York, NY) leaving an exposed window for exposure to the demineralization solution as shown in Fig. 1A. Each rectangular block fit precisely into an optomechanical assembly that could be positioned with micron accuracy.

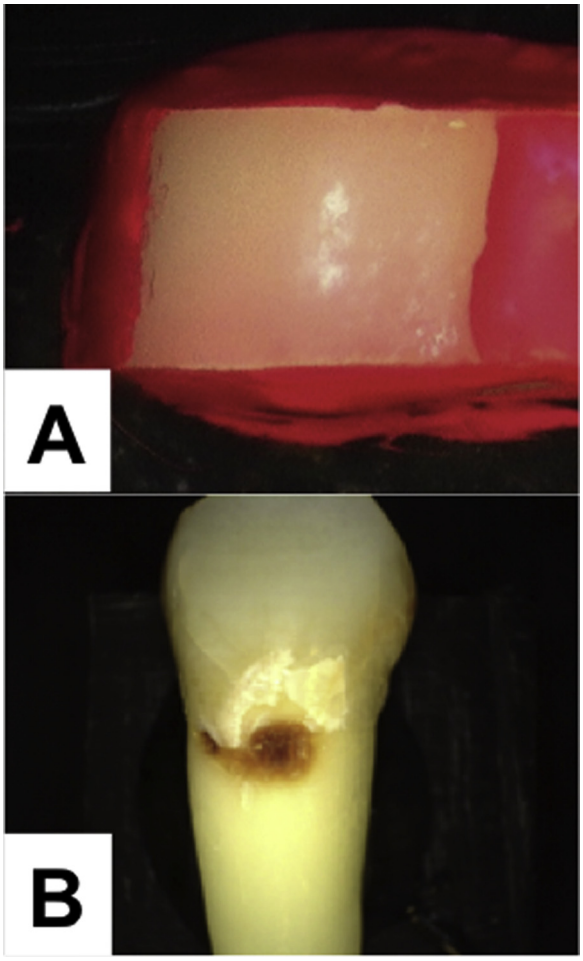

Fig. 1. Color images of (A) simulated or artificial lesion sample and (B) natural root caries lesion used in study.

Simulated active root caries lesions (surface-softened lesion model) were prepared in the exposed window using demineralization solution maintained at 37 °C at pH 4.9 [15]. The solution consists of 40 mL aliquots of 2.0 mmol/L phosphate, 2.0 mmol/L calcium, and 0.075 mol/L acetate. Twenty samples were placed in this solution for 7 days. After exposure the samples were taken from the solution, rinsed with deionized water, and stored in a 0.1% thymol solution for further examination.

In addition five natural root lesions on extracted teeth that manifested shrinkage were chosen for measurement. One of the teeth chosen is shown in Fig. 1B.

2.2. Cross-polarization optical coherence tomography (CP-OCT)

The cross-polarization OCT system used for this study was purchased from Santec (Komaki, Aichi, Japan). This system is shown in Fig. 2A and it acquires only the cross polarization image (CP-OCT), not both the cross and co-polarization images (PS-OCT). The Model IVS-3000-CP utilizes a swept laser source; Santec Model HSL-200-30 operating with a 30 kHz a-scan sweep rate. The Mac-Zehnder interferometer is integrated into the handpiece that also contains the microelectromechancial (MEMS) scanning mirror and the imaging optics. It is

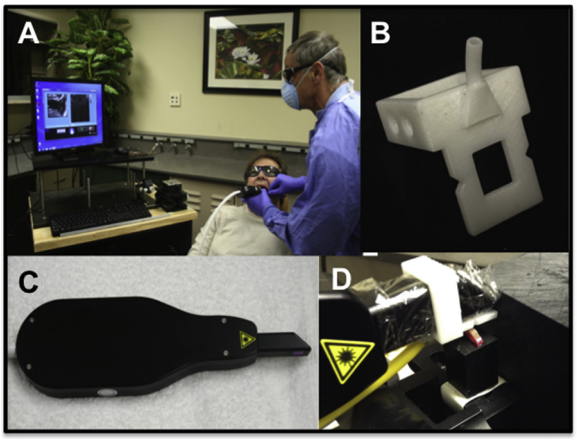

Fig. 2. (A) CP-OCT system, (B) 3D printed appliance with air nozzle, (C) CP-OCT scanning handpiece and (D) distal end of handpiece with attached appliance and polypropylene film for infection control.

capable of acquiring complete tomographic images of a volume of 6 × 6 × 7 mm in approximately three seconds. The distal end of the hand-piece is shown in Fig. 2D along with the appliance attached to the imaging end for dehydration. The body of the handpiece shown in Fig. 2C is 7 × 18 cm with an imaging tip that is 4 cm long and 1.5 cm across. This system operates at a wavelength of 1321-nm with a bandwidth of 111-nm with a measured resolution in air of 11.4 μm (3 dB). The lateral resolution is 80-μm ($1/e^2$) with a transverse imaging window of 6 mm × 6 mm and a measured imaging depth of 7-mm in air. The polarization extinction ratio was measured to be 32 dB.

We printed appliances that fit over the end of the CP-OCT scanner using a Formlabs 2 printer (Somerville, MA) that were printed using black, white and Dental SG resins. The Dental SG resin is autoclavable. An example of a printed appliance is shown in Fig. 2B. For infection control the entire CP-OCT handpiece is covered in polypropylene film and the appliance is placed over that film and the appliance is placed directly in contact with the tooth surface. All measurements were carried out with the handpiece covered in polypropylene film as shown in Fig. 2D as would be required for clinical use. A nozzle is attached to the appliance to provide air to both dehydrate the lesion area and prevent fogging of the scanning window when used *in vivo*.

2.3. Surface level changes for shrinkage assessment

Shrinkage measurements were taken using the Santec clinical OCT hand piece with the 3D-printed attachment, allowing for air-flow through a rectangular aperture directed across the surface of the sample to be scanned. Air-nozzle pressure was maintained at 20 psi for the duration of the drying process unless otherwise noted. The rate of shrinkage was also measured at 15 and 25 psi for comparison. Drying was typically done for 120 s and the sample was continuously scanned as a two-dimensional slice (b-scan image) in real time, and screen captured using Bandicam software (Seoul, Korea) during drying. The influence of the nozzle pressure (15, 20 and 25 psi) and the drying time (0, 30 and 120 s) on the shrinkage rate was also investigated.

The captured videos were then extracted and processed into frames. For the duration of 30 s, each video was recorded at 10 frames per second resulting in 300 total frames. These frames were then batch-imported into Matlab from Mathworks, Inc. (Natick, MA), in the form of images. Each image-frame was cropped to the lesion window and filtered using a Gaussian filter (5 × 5) to reduce noise. Surface detection was done using a Canny edge detection algorithm (threshold = [0.1 0.25]), revealing the surface line, and the level of this surface was arrayed for each frame. Any surface breaks, null or outlier, were resolved *via* interpolation to maintain consistency. The mean position of the lesion surface was recorded at each time point. The minimum average surface level was represented as 0, and the remaining surface levels were scaled with this in mind, resulting in a value representing the level of the surface at each time point.

The mean surface level for each time point was graphed with respect to time, revealing a consistent downward trend as can be seen in Fig. 3. Since the resulting graph is somewhat noisy, the data were fitted linearly to eliminate noise effects on the shrinkage measurement. The surface level difference between the linear fit at initial and final points was determined to find the overall shrinkage of the lesion window. The shrinkage rate in microns per second was calculated by taking the overall shrinkage and dividing by the total time elapsed.

2.4. Lesion thickness changes for shrinkage assessment and integrated reflectivity measurements

CP-OCT images were acquired of simulated and natural lesions after drying for 0, 30 and 120 s. Selected ranges of a-scans over the demineralized lesion windows were chosen for depth and reflectivity measurements. Areas of the sample which were found to be eroded were

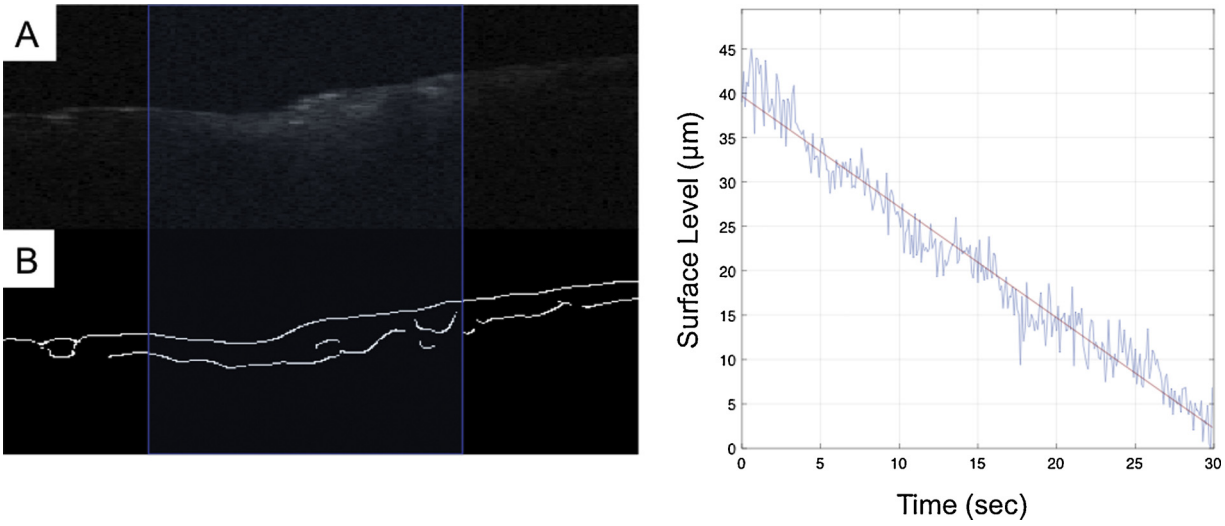

Fig. 3. (A) Raw CP-OCT image acquired of one of the natural root caries lesions along with the (B) processed image showing the detected edges after image processing. The relative change in the surface level or position (top edge) is plotted *versus* time during dehydration.

excluded from measurement. The width of the peak representing the depth of demineralization was measured for each condition and demarcated by a $1/e^2$ reduction in intensity compared to the maximum of that peak to yield the lesion thickness. The reflectivity of the subsurface peak was also integrated over the extent of the $1/e^2$ depth. The integrated reflectivity measurements were then divided by the depth by which they were calculated to yield a per micron reflectivity measurement, the integrated reflectivity per micron. All measurements were averaged over the lesion windows.

2.5. Statistical analysis

Repeated measures analysis of variance (RM-ANOVA) with Tukey-Kramer post-hoc multiple comparison test was used to compare the shrinkage rate, total shrinkage, lesion thickness, and integrated reflectivity per micron thickness for simulated and natural lesions at different airflow pressures and drying time with a significance level of 0.05. All statistical analysis was carried out using Prism from Graphpad Software (La Jolla, CA).

3. Results

3.1. Surface level changes for shrinkage assessment

A raw CP-OCT image acquired of one of the natural root caries lesions along with the processed image showing the detected edges after image processing is shown in Fig. 3. A plot of the relative change in the surface level or position (top edge) *versus* time during dehydration is also shown. The shrinkage rate and total shrinkage assessed by changes in surface position or level after 30 s of drying time for three different pressure settings for air flow are tabulated in Table 1. Variation in the pressure from 15 to 25 psi did not significantly increase the rate of shrinkage or the total shrinkage. The mean total shrinkage at 25 psi was 29-μm for the 7-day simulated lesions and 22-μm for the natural lesions. An unpaired *t*-test indicated that the difference between the two lesion types was significant ($P < 0.05$).

CP-OCT b-scan images for one of the simulated lesions and one of the natural lesions before and after drying are shown in Fig. 4. The shrinkage is quite small and cannot be easily detected by cursory examination of the images. However, the intensity of lesion areas is notably higher for the dry samples. A well defined transparent surface zone that is characteristic of arrested lesions is not visible on the natural lesion near the lesion surface which suggests that it is active [10–12].

3.2. Lesion thickness changes for shrinkage assessment and integrated reflectivity measurements

In addition to looking at changes in the surface level above the lesion area, the degree of shrinkage can be monitored by measuring changes in the thickness of the lesion. The lesion depth was monitored using CP-OCT before and after drying. The mean lesion thickness and the mean lesion integrated reflectivity are tabulated in Table 1 for the simulated and natural lesions. There was a significant decrease in the lesion thickness for both lesion types after 30 s. Drying the lesion for another 90 s at 20 psi did not yield a significant reduction in lesion thickness. The change in lesion thickness over 30 s of drying was 49.4-μm for the 7-day simulated lesions and 53-μm for the natural lesions. An unpaired *t*-test indicated that the difference was not significant ($P > 0.05$) between the two lesion types. The change in thickness assessed by measuring the lesion thickness was twice as high as it was for measuring the lesion surface level. There was a significant increase in the integrated reflectivity per micron thickness for both lesion types after 30 s. Drying the lesion for another 90 s at 20 psi did not yield a significant increase in the integrated reflectivity per micron thickness. The increase in the integrated reflectivity per micron thickness over 30 s of drying was 16.7% for the 7-day simulated lesions and 86.9% for

Table 1
Mean Shrinkage, lesion thickness and integrated reflectivity measurements before and after dehydration of the simulated and natural root caries lesions. Measurements in each section (row) of three with same letter are statistically similar $P > 0.05$.

	Total Shrinkage [μm] *vs* Pressure (psi)			Shrinkage Rate [μm/s] *vs* Pressure (psi)			Lesion Thickness [μm] *vs* Time Elapsed (sec)				Integrated Reflectivity per Micron Thickness [dB/μm] *vs* Time Elapsed (sec)			
	15	20	25	15	20	25	0	30	120		0	30	120	
Simulated (n = 20)	24.6 ± 10.6[a]	25.9 ± 9.7[a]	28.9 ± 9.3 [a]	0.81 ± 0.35[a]	0.86 ± 0.32[a]	0.96 ± 0.31[a]	223.3 ± 49.8[a]	173.9 ± 38.6[b]	165.2 ± 34.6[b]		2.34 ± 0.76[a]	2.73 ± 0.82[b]	3.09 ± 0.94[b]	
Natural (n = 5)	16.5 ± 10.3[a]	18.8 ± 13.9[a]	22 ± 14.6[a]	0.55 ± 0.34[a]	0.63 ± 0.46[a]	0.73 ± 0.49[a]	188.7 ± 40.4[a]	136.0 ± 19.1[b]	138.3 ± 24.1[b]		2.51 ± 0.52[a]	4.69 ± 1.25[b]	4.82 ± 1.34[b]	

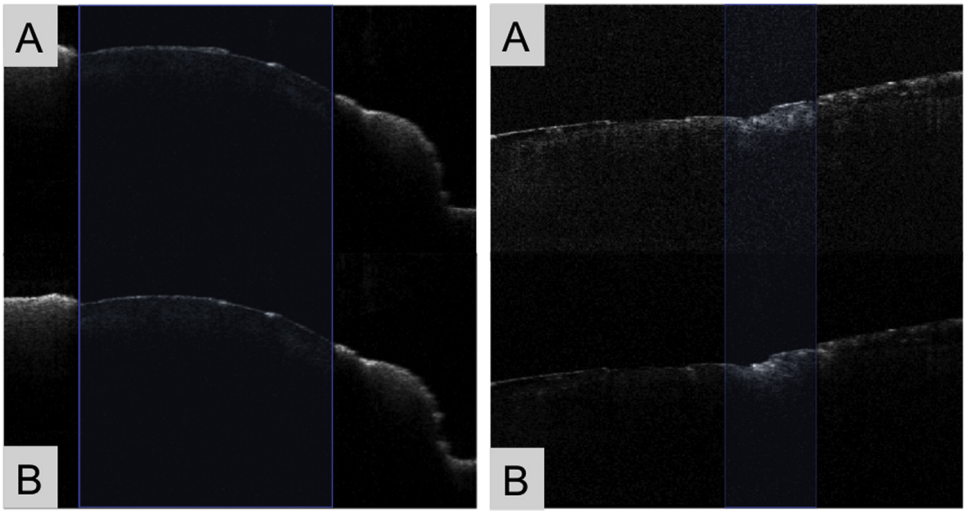

Fig. 4. Examples of CP-OCT b-scan images before (A) and after dehydration (B) from simulated (left) and natural (right) root caries lesions.

the natural lesions. An unpaired *t*-test indicated that the difference was significant ($P < 0.05$) between the two lesion types.

4. Discussion

In this study the shrinkage of both simulated and natural lesions on root surfaces was measured using a specially adapted CP-OCT handpiece with an attached appliance for dehydration and attached polypropylene film for infection control that is required for clinical use. It is important to include the polypropylene film in testing the device since the film interferes with the quality of the OCT images. The probe was designed to be used in contact with the tooth surface to minimize motion artifacts during *in vivo* use.

We choose to test the device on both simulated and natural lesions since there are limitations with both lesion types. The primary advantage of using simulated lesions is that the surface softened lesion model is reliable for producing active lesions. However, it is not clear how well the simulated root caries emulate natural lesions. The primary challenge in selecting natural lesions on extracted teeth is that there is no gold standard for lesion activity. Visual and tactile criteria are highly subjective. Therefore, we chose five lesions on extracted teeth that actually manifested shrinkage assuming that these lesions are active. There were no transparent surface zones visible in the CP-OCT scans for the selected lesions which provides further evidence that these lesions that manifest shrinkage are indeed active [10–12].

Two different approaches were used to measure shrinkage. In the first approach the contraction of the surface was measured by monitoring the surface position or the surface level during drying. This approach was successful in measuring significant changes after 30 s, however the shrinkage was significantly larger for the simulated lesions *versus* the natural lesions and the mean change was only 20–30 μm. The second approach was more promising and involved monitoring changes in the thickness of the lesion and the integrated reflectivity with depth during drying. There was a significant decrease in the lesion thickness and increase in the integrated reflectivity per micron of the lesion after drying for the natural lesions. Moreover, the changes were almost two times higher for lesion thickness and integrated reflectivity than they were for the surface level changes and they were greater for the natural lesions than for the simulated lesions suggesting that this approach has greater potential to be more sensitive clinically.

Shrinkage can potentially be used as a marker for lesion activity and to indicate that remineralization has taken place. Mineral deposition in the pores near the surface of the lesion during remineralization increases the mineral content near the surface and forms a surface layer. This highly mineralized surface layer reduces the permeability of fluids preventing water loss and shrinkage along with further demineralization and remineralization arresting lesion progression and repair. Traditional methods of visual-tactile diagnosis for root caries can result in a correct diagnosis, but often not until the lesion is at an advanced stage. Histological analyses for lesion activity assessment such as transverse microradiography (TMR) and polarized light microscopy (PLM) require destruction of the tooth and are not suitable for use *in-vivo*, while OCT is well suited for use *in-vivo*. Incorrect diagnosis can result in under treatment or over treatment. If a decision to restore is made prematurely when remineralization was feasible, the patient is committed to a restoration and often replacement restorations that become progressively larger. If the lesion is active and intervention is delayed, often the patient will require a more invasive and expensive restorative procedure.

5. Conclusions

In summary, we have demonstrated that a CP-OCT handpiece with an attached air nozzle can potentially be used for measurements of lesion permeability by monitoring the shrinkage of root caries lesion during drying with air. There was a significant contraction of the lesion surface, significant decrease in the lesion thickness and increase in the reflectivity per micron from the lesion upon drying simulated and natural lesions. In addition, we have developed a new approach for measuring lesion shrinkage with OCT, namely monitoring changes in the lesion thickness as opposed to the position of the lesion surface that does not require an initial reference position and is more easily implemented *in vivo*.

Declaration of Competing Interest

The authors have no relevant financial interests in this article and no potential conflicts of interest to disclose.

Acknowledgments

This work was supported by NIH/NIDCR Grant R01-DE027335 and TRDRP Grant 27IP-0015.

References

[1] D.W. Banting, Diagnosis of Root Caries, NIH Diagnosis and Management of Dental Caries Throughout Life, NIH Consensus Statement, (2001), pp. 1–24.
[2] D.W. Banting, Diagnosis and prediction of root caries, Adv. Dent. Res. 7 (2) (1993) 80–86.

[3] P. Hellyer, D. Beighton, M. Heath, E. Lynch, Root caries in older people attending a general practice in East Sussex, Br. Dent. Nurs. J. 169 (1990) 201–206.
[4] M. Schaeken, H. Keltjens, J. Van der Hoeven, Effects of fluoride and chlorhexidine on the microflora of dental root surfaces and progression of root-surface caries, J. Dent. Res. 70 (191) (1991) 150–153.
[5] K. Ekstrand, S. Martignon, P. Holm-Pedersen, Development and evaluation of two root caries controlling programmes for home-based frail people older than 75 years, Gerodontology 25 (2) (2008) 67–75.
[6] O. Fejerskov, W.M. Luan, B. Nyvad, E. Budtz-Jorgensen, P. Holm-Pedersen, Active and inactive root surface caries lesions in a selected group of 60- to 80-year-old Danes, Caries Res. 25 (5) (1991) 385–391.
[7] A. Ismail, D. Banting, H. Eggertsson, K. Ekstrand, A. Ferreira-Zandona, C. Longbottom, N. Pitts, E. Reich, D. Ricketts, R. Selwitz, W. Sohn, G. Topping, D. Zero, Rationale and evidence for the International Caries Detection and Assessment System (ICDAS II), in: G.K. Stookey (Ed.), Proceedings of the 7th Indiana Conference, Indianapolis: Indiana University, 2005, pp. 161–221.
[8] N. Pitts, Detection, assessment, diagnosis and monitoring of caries, in: A.L. Whitforn (Ed.), Monographs in Oral Science, Karger, Basel, 2009.
[9] E. Lynch, D. Beighton, A comparison of primary root caries lesions classified according to colour, Caries Res. 28 (4) (1994) 233–239.
[10] R.S. Jones, C.L. Darling, J.D. Featherstone, D. Fried, Remineralization of in vitro dental caries assessed with polarization-sensitive optical coherence tomography, J. Biomed. Optics 11 (1) (2006) 014016.
[11] R.S. Jones, D. Fried, Remineralization of enamel caries can decrease optical reflectivity, J. Dent. Res. 85 (9) (2006) 804–808.
[12] S.K. Manesh, C.L. Darling, D. Fried, Nondestructive assessment of dentin demineralization using polarization-sensitive optical coherence tomography after exposure to fluoride and laser irradiation, J. Biomed. Mater. Res. B Appl. Biomater. 90 (2) (2009) 802–812.
[13] H. Kang, C.L. Darling, D. Fried, Nondestructive monitoring of the repair of enamel artificial lesions by an acidic remineralization model using polarization-sensitive optical coherence tomography, Dent. Mater. 28 (5) (2012) 488–494.
[14] B.T. Amaechi, A.G. Podoleanu, G. Komarov, S.M. Higham, D.A. Jackson, Quantification of root caries using optical coherence tomography and microradiography: a correlational study, Oral Health Prev. Dent. 2 (4) (2004) 377–382.
[15] C. Lee, C. Darling, D. Fried, Polarization sensitive optical coherence tomographic imaging of artificial demineralization on exposed surfaces of tooth roots, Dent. Mater. 25 (6) (2009) 721–728.
[16] S.K. Manesh, C.L. Darling, D. Fried, Polarization-sensitive optical coherence tomography for the nondestructive assessment of the remineralization of dentin, J. Biomed. Optics 14 (4) (2009) 044002.
[17] I. Wada, Y. Shimada, M. Ikeda, A. Sadr, S. Nakashima, J. Tagami, Y. Sumi, Clinical assessment of non carious cervical lesion using swept-source optical coherence tomography, J. Biophotonics 8 (10) (2015) 846–854.
[18] K. Kaneko, K. Matsuyama, S. Nakashima, Quantification of early carious enamel lesions by using an infrared camera, in: G.K. Stookey (Ed.), Early Detection of Dental Caries II, Indiana University, Indianapolis, IN, 1999, pp. 83–99.
[19] C.M. Zakian, A.M. Taylor, R.P. Ellwood, I.A. Pretty, Occlusal caries detection by using thermal imaging, J. Dent. 38 (10) (2010) 788–795.
[20] R.C. Lee, C.L. Darling, D. Fried, Assessment of remineralization via measurement of dehydration rates with thermal and near-IR reflectance imaging, J. Dent. 43 (2015) 1032–1042.
[21] R.C. Lee, C.L. Darling, D. Fried, Activity assessment of root caries lesions with thermal and near-infrared imaging methods, J. Biophotonics 10 (3) (2016) 433–445.
[22] V.B. Yang, D.A. Curtis, D. Fried, Use of Optical Clearing Agents for Imaging Root Surfaces with Optical Coherence Tomography, J. Sel. Topics Quant. Elect. 25 (1) (2018) 1–7.